Acta Crystallographica Section F
Structural Biology and Crystallization Communications
ISSN 1744-3091

Structure of the first PDZ domain of human PSD-93

Monica Fiorentini, Ann Kallehauge Nielsen, Ole Kristensen, Jette S. Kastrup and Michael Gajhede*

Biostructural Research, Department of Medicinal Chemistry, Faculty of Pharmaceutical Sciences, University of Copenhagen, Universitetsparken 2, DK-2100 Copenhagen, Denmark

Correspondence e-mail: mig@farma.ku.dk

Received 31 August 2009
Accepted 20 October 2009

PDB Reference: PSD-93 PDZ1 domain, 2wl7, r2wl7sf.

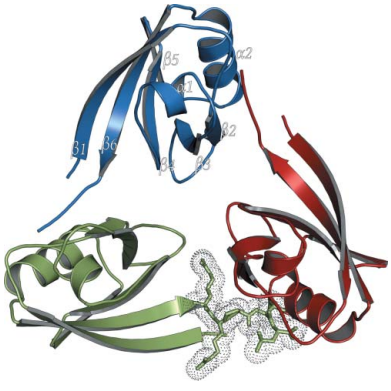

The crystal structure of the PDZ1 domain of human PSD-93 has been determined to 2.0 Å resolution. The PDZ1 domain forms a crystallographic trimer that is also predicted to be stable in solution. The main contributions to the stabilization of the trimer seem to arise from interactions involving the PDZ1–PDZ2 linker region at the extreme C-terminus of PDZ1, implying that the oligomerization that is observed is not of biological significance in full-length PSD-93. Comparison of the structures of the binding cleft of PSD-93 PDZ1 with the previously reported structures of PSD-93 PDZ2 and PDZ3 as well as of the closely related human PSD-95 PDZ1 shows that they are very similar in terms of amino-acid composition. However, the cleft is significantly narrower in PSD-95. This could be part of the basis of peptide selectivity between PSD-93 PDZ1 and PSD-95 PDZ1.

1. Introduction

The human family of membrane-associated guanylate kinase (MAGUK) proteins comprises four members named PSD-93 (DLG2, Chapsyn-110), PSD-95 (SAP90), SAP97 (hdlg) and SAP102. These proteins are key components of the postsynaptic density (PSD) and are known to play important roles in synaptic localization and clustering of ionotropic glutamate receptors (iGluRs; Elias & Nicoll, 2007). They are consequently also implicated in CNS disorders (Gardoni *et al.*, 2009), making the development of specific pharmacological tools an important overall goal.

All MAGUK proteins contain three N-terminal PDZ domains (PDZ1–PDZ3), an SH3 domain and a guanylate kinase domain. The PDZ domains of MAGUK proteins are known to interact with the outermost carboxy-terminal ends of iGluRs. Binding of the carboxy-termini of proteins involved in intracellular signalling is the general function of the more than 1000 PDZ domains encoded by the human genome (Jeleń *et al.*, 2003). PDZ domains contain six β-strands and two α-helices that form a β-sandwich. The binding groove is located between the β2 strand and the α2 helix and harbours residues of importance for specificity towards different binding partners. The PDZ domains have been divided into four classes based on the carboxy-terminal sequences of their binding partners (Songyang *et al.*, 1997). Class I has a consensus binding sequence -*X*-(S/T)-*X*-φ as found in, for example, the NMDA-type iGluRs and the metabotropic glutamate receptor mGluR5. Recent investigations have shown that this classification scheme is oversimplified as affinity differences within the classes can be very large (Stiffler *et al.*, 2007) and consequently more rigorous classification schemes have been introduced that are based on comparisons of the ten carboxy-terminal residues of the interacting proteins (Tonikian *et al.*, 2008).

It has been well established that the most studied MAGUK protein PSD-95 binds to the NR2A and NR2B subtypes of NMDA receptors, which have identical carboxy-terminal sequences (SIEDSV; Lim *et al.*, 2002; Stiffler *et al.*, 2007; Tonikian *et al.*, 2008). Studies using PSD-95 knockout mice and shRNA interference have also shown that PSD-95 is important for AMPA receptor responses (Elias *et al.*, 2006). The three-dimensional structures of all three PSD-95 PDZ domains have been determined (Doyle *et al.*, 1996; Long *et al.*, 2003; Tochio *et al.*, 2000) and the structure of a complex of PSD-95 PDZ3 and a class

I peptide (TKNTKQTSV) established a canonical binding mode (Doyle *et al.*, 1996). One notable feature of this mode is that the terminal carboxylate O atoms of the bound peptide interact with three backbone N atoms of the PDZ domain and a water molecule but not with any side-chain atoms. Measurements using the fluorescent polarization technique have established K_d values in the low micromolar range between an NR2B peptide and both PSD-95 PDZ1 and PDZ2 (20 and 3 μ*M*, respectively), whereas no affinity was observed for the PDZ3 domain (Bach *et al.*, 2008). Slightly lower K_d values towards the NR2B peptide were observed when using a construct comprising both PSD-95 PDZ1 and PDZ2.

PSD-93 is very similar to PSD-95 in terms of amino-acid sequence, domain organization, developmental expression and function (Elias *et al.*, 2006), but differences in expression profiles have been observed. Cerebellar Purkinje cells have been shown to be enriched in PSD-93 (Cheng *et al.*, 2006). Similarly, the delta-2 receptor that was discovered in 1992 (Yamazaki *et al.*, 1992) as a member of the iGluR family is also expressed in these cells. It has still not been possible to identify an endogenous ligand that can activate the delta-2 receptor (Schmid & Hollmann, 2008), even though it has been established that the receptor is capable of binding D-serine and glycine in the ligand-binding domain (Naur *et al.*, 2007). Despite this, it has been shown that removal of the seven carboxy-terminal residues of the receptor results in impaired long-term depression, a phenomenon that is central to memory and learning (Kakegawa *et al.*, 2008; Kohda *et al.*, 2007).

PSD-93, as well as PSD-95, has been shown to have affinity for the delta-2 receptor using yeast two-hybrid and immunoprecipitation techniques (Roche *et al.*, 1999). It was further shown that the interactions were dependent on the delta-2 carboxy-terminal residues DRGTSI. The structures of the second and third PDZ domains of PSD-93 have been reported previously (Elkins *et al.*, 2007). As a first step towards investigating the interactions between delta-2 and PSD-93 at the molecular level, we have determined the structure of the PSD-93 PDZ1 domain.

2. Materials and methods

2.1. Construct design and subcloning

The PSD-93 and PSD-95 sequences were aligned in *ClustalW* (Larkin *et al.*, 2007), revealing significant sequence identity in the region of the PDZ1 domains of the proteins and above 95% conservation among orthologous mammalian sequences. To define the boundaries of the PSD-93 PDZ1 domain, structural alignments of the PDZ domains were performed using the program *TCoffee* (O'Sullivan *et al.*, 2004) with at least ten extra residues added to the predicted PDZ1 boundaries of PSD-93. The PSD-93 PDZ1 domain was individually aligned with 15 PDZ domains of known structure in the *TCoffee* regular Expresso mode. Secondary-structural elements were deduced according to how the residues of the PSD-93 PDZ1 domain individually aligned in *TCoffee* with residues implicated in β-strand formation. PSD-93 cDNA was obtained from Open Biosystems (Huntsville, Alabama, USA) as a synthetic mouse ORF from the Mammalian Gene Collection (Image Consortium Clone ID 100015000) in pENTR223.1 vector and was used as a template to PCR-amplify the PDZ1 domain (forward primer, 5′-AAAGAATTCGAATTTGAAGAAATTACATTGGAGA-3′; reverse primer, 5′-AAAGCGGCCGCTCACAATATGGGT-3′). The amplified PCR product encoding residues 97–190 of PSD-93 was subcloned into the *Eco*RI/*Not*I cloning sites of the pGEX-6P-1 plasmid (GE Healthcare) using XL1-Blue Supercompetent cells (Stratagene) for transformation and selection of positive colonies. The construct was verified by DNA sequencing (Eurofins MWG Operon, Germany).

Table 1
Data-collection and refinement statistics.

Data collection	
X-ray source	Rotating anode
Wavelength (Å)	1.5418
Space group	*R*3(*H*)
Unit-cell parameters	
a (Å)	85.2
b (Å)	85.2
c (Å)	45.5
Resolution (Å)	28–2.01 (2.12–2.01)
No. of unique observations	7993 (1019)
Redundancy	11.2 (10.6)
Completeness (%)	97.9 (85.8)
$I/\sigma(I)$	27.2 (8.2)
R_{merge}† (%)	7.1 (31.2)
Refinement	
R_{conv}‡ (%)	16.4
R_{free}§ (%)	20.8
R.m.s.d., bond lengths (Å)	0.003
R.m.s.d., bond angles (°)	0.7
Mean *B* factor (Å^2)	19.4

† $R_{merge} = \sum_{hkl}\sum_i |I_i(hkl) - \langle I(hkl)\rangle| / \sum_{hkl}\sum_i I_i(hkl)$, where $I_i(hkl)$ is the intensity of an individual measurement of the reflection with Miller indices *hkl* and $\langle I(hkl)\rangle$ is the mean intensity of that reflection. ‡ $R_{conv} = \sum_{hkl} ||F_{obs}| - |F_{calc}|| / \sum_{hkl} |F_{obs}|$, where $|F_{obs}|$ and $|F_{calc}|$ are the observed and calculated structure-factor amplitudes. § R_{free} is equivalent to R_{conv} but calculated with reflections omitted from the refinement process (10% of reflections were omitted).

2.2. Protein production and crystallization

Plasmid DNA was introduced into *Escherichia coli* BL21 (DE3) pLysS cells (Novagen); when the culture reached an OD_{600} of 0.6 in Luria–Bertani medium, induction was carried out overnight at 298 K by adding 0.5 m*M* isopropyl β-D-1-thiogalactopyranoside (Sigma). The protein was produced as a GST-fusion protein and purified by affinity chromatography after cell disruption (Constant Systems Ltd, England) using a GSTrap FF affinity column (GE Healthcare). The affinity tag was removed by overnight incubation at 277 K with PreScission protease (1 U per milligram of fusion protein). The protein was further purified using gel filtration (Superdex 75 HR, GE Healthcare) in PBS buffer. PSD-93 PDZ1-containing fractions were concentrated to 1.7 mg ml^{-1} by centrifugal filtration (Amicon Ultra-4). Protein crystallization was performed in hanging-drop vapour-diffusion experiments by mixing 1 μl protein solution and 1 μl reservoir solution (0.01 *M* nickel chloride hexahydrate, 0.1 *M* Tris–HCl pH 8.5, 1.0 *M* lithium sulfate). Crystals were obtained within 2 d at room temperature.

2.3. Crystallographic methods

X-ray data were collected at 100 K from a cryoprotected crystal (reservoir solution containing 20% sucrose) using Cu *Kα* radiation from a Rigaku 200 rotating-anode generator equipped with Osmic focusing mirrors and a MAR 345 detector. The data were indexed, integrated and scaled using the *CCP*4 programs *MOSFLM* and *SCALA* (Collaborative Computational Project, Number 4, 1994). Crystal data and data-collection statistics are listed in Table 1.

The PDZ1 structure was determined by the molecular-replacement method using the program *Phaser* (McCoy *et al.*, 2007). The crystal structure of PSD-95 PDZ1 (PDB code 1iu0, molecule *A*; Long *et al.*, 2003) was used as a search model and a convincing solution accounting for the single molecule in the asymmetric unit was obtained. Subsequently, automated model building was performed using the program *ARP*/*wARP* (Langer *et al.*, 2008). This resulted in

tracing of 95% of the residues. The missing residues were inserted manually using the program *Coot* (Emsley & Cowtan, 2004). Structure refinement was performed with the *PHENIX* program package (Adams *et al.*, 2002). Water molecules, three sulfate ions and one chloride ion were gradually introduced into the structure. The quality of the structure was evaluated using the program *PROCHECK* (Laskowski *et al.*, 1993). Figures were prepared using the program *PyMOL* (DeLano, 2002).

3. Results and discussion

3.1. Overall structure of PSD-93 PDZ1

One PSD-93 PDZ1 molecule is found in the asymmetric unit of the crystal. All residues but Asn156 (which has very well defined electron density) are in the allowed regions of the Ramachandran plot. Each PSD-93 PDZ1 domain contains eight segments of secondary structure (Fig. 1), as expected (Jeleń *et al.*, 2003). Six β-strands and two α-helices form a β-sandwich, with one strand participating in both sheets. As expected from the high degree of sequence identity (53 and 44%) to the PSD-93 PDZ2 and PSD-93 PDZ3 domains, these structures also superimpose well on the PDZ1 domain, with r.m.s. deviations on backbone C^{α} atoms of 0.59 and 0.64 Å, respectively.

The structure of PSD-93 PDZ1 also superimposes very well with the structure of PSD-95 PDZ3 bound to the CRIPT peptide TKNTKQTSV. 13 residues in PSD-93 PDZ1 are located within 4 Å of the CRIPT peptide. Thus, residues Arg105, Leu110, Gly111, Phe112, Ser113, Ile114, Ala115, Gly116, Asn120, Thr132, His165, Val169 and Leu172 define a canonical class I peptide-binding groove in PSD-93 PDZ1. All but two residues are conserved with all atoms at very similar spatial positions in the PSD-93 PDZ1, PDZ2 and PDZ3 domains, including PDZ1 His165, which is important for hydrogen bonding to the Ser/Thr at the peptide −2 position. The exceptions are Arg105, which is a lysine residue in PSD-93 PDZ2 and PDZ3, and Ala115, which is a valine in PDZ3. These similarities suggest quite similar affinities of the three PSD-93 PDZ domains towards class I peptides. All binding-site residues are conserved in the PDZ1 domains of PSD-93 and PSD-95.

3.2. PSD-93 PDZ1 oligomeric structure

PSD-93 PDZ1 is seen to form a trimer in the crystal (Fig. 1). The three modules are related by a crystallographic threefold axis. The *PISA* server (Krissinel & Henrick, 2007) predicts the trimer to be stable in solution, which is in agreement with the results of size-exclusion chromatography (data not shown). PDZ–PDZ oligomerization is unusual but has been described for the tandem domains of syntenin (Kang *et al.*, 2003). The interactions did not involve the carboxy-terminus of the truncated proteins; however, the contact surface was relatively small.

The trimer interactions include the PDZ1 peptide-binding cleft as the carboxy tails –RRRPIL of the monomers occupy the binding clefts of adjacent molecules. The details of the interactions are shown in Fig. 2. Hydrogen-bonding interactions are seen with the backbone N atoms of the GLGF motif (RLGF in PSD-93 PDZ1). These interactions are similar to those observed for canonical PDZ peptide binding in the structure of PSD-95 PDZ3 bound to the peptide KKETWV (PDB code 1tp5; D. Saro, Z. Wawrzak, P. Martin, J. Vickrey, A. Paredes, L. Kovari & M. Spaller, unpublished work). However, significant differences are also observed. While it is the terminal carboxylate O atoms that form hydrogen bonds to these backbone N atoms in canonical binding, in PSD-93 PDZ1 one of the carboxylate O atoms of Leu190 and the backbone O atom of Ile189 are engaged in hydrogen-bond formation to the backbone N atoms of Leu110 and Gly111. The other carboxylate O atom forms a salt bridge to Arg105. Arg105 is a key residue as its side chain interacts directly with the carboxy-terminus of a bound peptide and it further functions to sterically close the binding groove at one end and to fix the position of helix α2 by interactions with the backbone carbonyl O atoms of

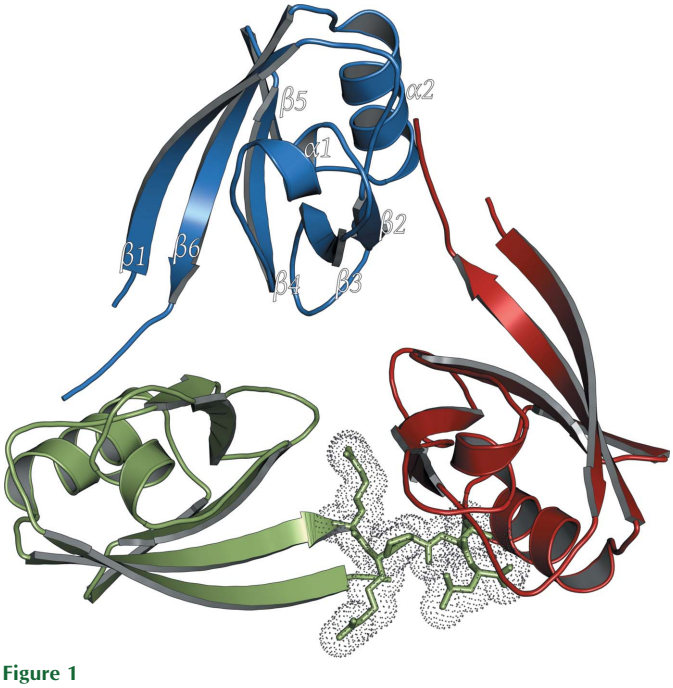

Figure 1
PSD-93 PDZ1 forms a crystallographic trimeric oligomer. The protein–protein interactions are primarily formed by docking of the C-terminal end of one PDZ1 molecule (dotted surface) into the binding groove of an adjacent PDZ1 molecule.

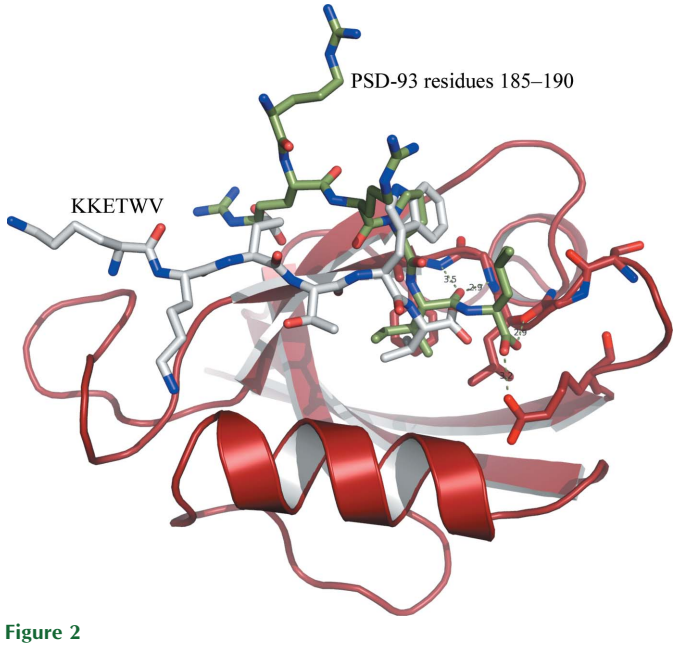

Figure 2
The binding cleft of PSD-93 PDZ1. PSD-93 PDZ1 is shown in red cartoon representation with key binding-site residues in stick representation. The binding of the carboxy-terminal end of an adjacent molecule from the trimer (shown in green C-atom stick representation) is seen to differ from the class 1 canonical peptide-binding mode (KKETWV peptide shown in grey C-atom stick representation; from the PSD-95 PDZ3–KKETWV complex; PDB code 1tp5).

Leu172 and Gly176 (not shown). Further affinity is gained as Ile189 occupies a hydrophobic cavity. A corresponding cavity in the PSD-95 PDZ3–KKETWV complex is occupied by the side chain of the terminal valine. Additional affinity arises from protein–protein interactions that do not involve the carboxy-terminus. The following residues are in van der Waals contact with an adjacent PDZ1 molecule: Glu95, Ile123, Gly124, Asp125, Asp126, Arg147, Val148 and Asn149. However, the main contributions to the stabilization of the trimer seem to arise from interactions involving the PDZ1–PDZ2 linker region at the extreme C-terminus, in particular the charged terminal carboxy group. This carboxy group is condensed to a peptide link in full-length PSD-93 and consequently cannot engage in trimer formation. In conclusion, this implies that the oligomerization observed is not of biological significance in full-length PSD-93.

3.3. Comparison with PSD-95 PDZ1

Comparison of PSD-93 PDZ1 and PSD-95 PDZ1 shows that the two domains are very similar overall. They superimpose with an r.m.s. deviation of 1.4 Å on C^{α} atoms. The largest deviations are observed between the two long α2 helices; the helix in PSD-95 PDZ1 is closer to the sheet, thus causing a significantly narrower binding cavity than that in PSD-93 PDZ1. This suggests that the PDZ1 domain of PSD-93 might accept peptides with larger residues in the C-terminus than PSD-95. The C-terminal residue of delta-2 is an isoleucine, which is bulkier than the valine found at the C-terminus of NMDA receptors. Therefore, this suggests that the PSD-93 PDZ1 domain could have higher affinity towards the delta-2 receptor than the PSD-95 PDZ1 domain and that PSD-93 specifically interacts with delta-2 in Purkinje cells.

The University of Copenhagen GluTarget programme of excellence (http://www.glutarget.dk) and the Danish Medical Research Council are acknowledged for financial support.

References

Adams, P. D., Grosse-Kunstleve, R. W., Hung, L.-W., Ioerger, T. R., McCoy, A. J., Moriarty, N. W., Read, R. J., Sacchettini, J. C., Sauter, N. K. & Terwilliger, T. C. (2002). *Acta Cryst.* D**58**, 1948–1954.

Bach, A., Chi, C. N., Olsen, T. B., Pedersen, S. W., Røder, M. U., Pang, G. F., Clausen, R. P., Jemth, P. & Strømgaard, K. (2008). *J. Med. Chem.* **51**, 6450–6459.

Cheng, D., Hoogenraad, C. C., Rush, J., Ramm, E., Schlager, M. A., Duong, D. M., Xu, P., Wijayawardana, S. R., Hanfelt, J., Nakagawa, T., Sheng, M. & Peng, J. (2006). *Mol. Cell. Proteomics*, **5**, 1158–1170.

Collaborative Computational Project, Number 4 (1994). *Acta Cryst.* D**50**, 760–763.

DeLano, W. L. (2002). *PyMOL Molecular Viewer.* http://www.pymol.org.

Doyle, D. A., Lee, A., Lewis, J., Kim, E., Sheng, M. & MacKinnon, R. (1996). *Cell*, **85**, 1067–1076.

Elias, G. M., Funke, L., Stein, V., Grant, S. G., Bredt, D. S. & Nicoll, R. A. (2006). *Neuron*, **52**, 307–320.

Elias, G. M. & Nicoll, R. A. (2007). *Trends Cell Biol.* **17**, 343–352.

Elkins, J. M., Papagrigoriou, E., Berridge, G., Yang, X., Phillips, C., Gileadi, C., Savitsky, P. & Doyle, D. A. (2007). *Protein Sci.* **16**, 683–694.

Emsley, P. & Cowtan, K. (2004). *Acta Cryst.* D**60**, 2126–2132.

Gardoni, F., Marcello, E. & Di Luca, M. (2009). *Neuroscience*, **158**, 324–333.

Jeleń, F., Oleksy, A., Śmietana, K. & Otlewski, J. (2003). *Acta Biochim. Pol.* **50**, 985–1017.

Kakegawa, W., Miyazaki, T., Emi, K., Matsuda, K., Kohda, K., Motohashi, J., Mishina, M., Kawahara, S., Watanabe, M. & Yuzaki, M. (2008). *J. Neurosci.* **28**, 1460–1468.

Kang, B. S., Cooper, D. R., Jelen, F., Devedjiev, Y., Derewenda, U., Dauter, Z., Otlewski, J. & Derewenda, Z. S. (2003). *Structure*, **11**, 459–468.

Kohda, K., Kakegawa, W., Matsuda, S., Nakagami, R., Kakiya, N. & Yuzaki, M. (2007). *Eur. J. Neurosci.* **25**, 1357–1362.

Krissinel, E. & Henrick, K. (2007). *J. Mol. Biol.* **372**, 774–797.

Langer, G., Cohen, S. X., Lamzin, V. S. & Perrakis, A. (2008). *Nature Protoc.* **3**, 1171–1179.

Larkin, M. A., Blackshields, G., Brown, N. P., Chenna, R., McGettigan, P. A., McWilliam, H., Valentin, F., Wallace, I. M., Wilm, A., Lopez, R., Thompson, J. D., Gibson, T. J. & Higgins, D. G. (2007). *Bioinformatics*, **23**, 2947–2948.

Laskowski, R. A., MacArthur, M. W., Moss, D. S. & Thornton, J. M. (1993). *J. Appl. Cryst.* **26**, 283–291.

Lim, I. A., Hall, D. D. & Hell, J. W. (2002). *J. Biol. Chem.* **277**, 21697–21711.

Long, J. F., Tochio, H., Wang, P., Fan, J. S., Sala, C., Niethammer, M., Sheng, M. & Zhang, M. (2003). *J. Mol. Biol.* **327**, 203–214.

McCoy, A. J., Grosse-Kunstleve, R. W., Adams, P. D., Winn, M. D., Storoni, L. C. & Read, R. J. (2007). *J. Appl. Cryst.* **40**, 658–674.

Naur, P., Hansen, K. B., Kristensen, A. S., Dravid, S. M., Pickering, D. S., Olsen, L., Vestergaard, B., Egebjerg, J., Gajhede, M., Traynelis, S. F. & Kastrup, J. S. (2007). *Proc. Natl Acad. Sci. USA*, **104**, 14116–14121.

O'Sullivan, O., Suhre, K., Abergel, C., Higgins, D. G. & Notredame, C. (2004). *J. Mol. Biol.* **340**, 385–395.

Roche, K. W., Ly, C. D., Petralia, R. S., Wang, Y. X., McGee, A. W., Bredt, D. S. & Wenthold, R. J. (1999). *J. Neurosci.* **19**, 3926–3934.

Schmid, S. M. & Hollmann, M. (2008). *Mol. Neurobiol.* **37**, 126–141.

Songyang, Z., Fanning, A. S., Fu, C., Xu, J., Marfatia, S. M., Chishti, A. H., Crompton, A., Chan, A. C., Anderson, J. M. & Cantley, L. C. (1997). *Science*, **275**, 73–77.

Stiffler, M. A., Chen, J. R., Grantcharova, V. P., Lei, Y., Fuchs, D., Allen, J. E., Zaslavskaia, L. A. & MacBeath, G. (2007). *Science*, **317**, 364–369.

Tochio, H., Hung, F., Li, M., Bredt, D. S. & Zhang, M. (2000). *J. Mol. Biol.* **295**, 225–237.

Tonikian, R. *et al.* (2008). *PLoS Biol.* **6**, e239.

Yamazaki, M., Araki, K., Shibata, A. & Mishina, M. (1992). *Biochem. Biophys. Res. Commun.* **183**, 886–892.